Am J Cancer Res 2016;6(5):894-909
www.ajcr.us /ISSN:2156-6976/ajcr0026357

Original Article

Simultaneous targeting of 5-LOX-COX and ODC block NNK-induced lung adenoma progression to adenocarcinoma in A/J mice

Gaurav Kumar[1*], Jagan Mohan R Patlolla[1*], Venkateshwar Madka[1], Altaf Mohammed[1], Qian Li[1], Yuting Zhang[1], Laura Biddick[1], Anil Singh[1], Allison Gillaspy[2], Stanley Lightfoot[1], Vernon E Steele[2], Levy Kopelovich[2], Chinthalapally V Rao[1]

[1]*Center for Cancer Prevention and Drug Development, Hematology-Oncology Section, Department of Medicine, Stephenson Cancer Center, University of Oklahoma Health Sciences Center, Oklahoma City, OK 73104, USA;* [2]*Division of Cancer Prevention, Chemoprevention Agent Development Research Group, National Cancer Institute, Bethesda, MD, USA.* [*]*Equal contributors.*

Received February 21, 2016; Accepted March 2, 2016; Epub May 1, 2016; Published May 15, 2016

Abstract: Lung cancer is the leading cause of cancer deaths worldwide. Targeting complementary pathways will achieve better treatment efficacy than a single agent high-dose strategy that could increase risk of side effects and tumor resistance. To target COX-2, 5-LOX, and ODC simultaneously, we tested the effects of a dual 5-LOX-COX inhibitor, licofelone, and an ODC inhibitor, DFMO, alone and in combination, on NNK-induced lung tumors in female A/J mice. Seven-week-old mice were treated with NNK (10 μmol/mouse, single dose, i.p.) and randomized to different treatment groups. Three weeks after injection, mice were fed control or experimental diets (DFMO 1500/3000 ppm, licofelone 200/400 ppm, or a low-dose combination of 1500 ppm DFMO and 200 ppm licofelone) for 17 or 34 weeks. Both agents significantly inhibited tumor formation in a dose-dependent manner. As anticipated more adenomas and adenocarcinomas were observed at 17 and 34 weeks, respectively. Importantly, low dose combination of DFMO and licofelone showed more pronounced effects at 17 or 34 weeks in inhibiting the total tumor formation (~60%, $p < 0.0001$) and adenocarcinoma (~65%, $p < 0.0001$) compared to individual high dose of DFMO (~44% and 46%, $p < 0.0001$) and licofelone (~48% and 55%, $p < 0.0001$). DFMO and combination-treated mice lung tumors exhibited modulated ODC pathway components (Oat, Oaz, SRM, SMS, and SAT, $p < 0.05$) along with decreased proliferation (PCNA, Cyclin D1 and Cyclin A) and increased expression of p53, p21 and p27 compared to mice fed control diet. Both DFMO and licofelone significantly inhibited tumor inflammatory markers. Our findings suggest that a low-dose combined treatment targeting inflammation and polyamine synthesis may provide effective chemoprevention.

Keywords: Lung cancer, chemoprevention, DFMO, licofelone, ornithine decarboxylase, Cox-2

Introduction

Lung cancer is the primary cause of cancer deaths in the US and worldwide: the 5-year survival rate is only 15% [1]. Eighty-five percent of cases of lung cancer can be attributed to tobacco smoking [1]. Tens of millions of smokers are at high risk for developing this malignancy. Although there has been a modest improvement in survival, the advances observed in other malignancies have not translated to lung cancer. The marked lethality of this disease is likely due to the high frequency of advanced stage at diagnosis and the disease's inherent therapeutic resistance. With advances in biologically targeted therapeutic agents, treatment of advanced lung cancer should continue to improve [2], but early diagnosis and effective chemopreventive interventions are crucial. Thus, intervention strategies and effective chemopreventive approaches targeting early lesions, adenoma, and adenocarcinoma may be useful for high-risk ex-smokers or those who are diagnosed with lung adenomas [3].

Clinical and preclinical studies have demonstrated that eflornithine (DFMO) is a potential chemopreventive agent [4-7]. The rationale for the use of DFMO, an ornithine decarboxylase (ODC) inhibitor, as a cancer chemopreventive agent has been strengthened over the years

because ODC is found to be activated in cancer, which is followed by an increase in concentrations of the polyamines putresine, spermine, and spermidine that are associated with tumor promotion and progression. ODC is also modulated by important genes of the polyamine biosynthesis pathway, such as arginase (Arg1), ornithine aminotransferase (Oat), ODC antizyme (Oaz), and spermidine/spermine N(1)-acetyltransferase (SAT1). A link between polyamine levels and tumor grade and stage is well established [8, 9]. Some studies have reported that lung carcinomas have greatly elevated polyamine levels [10, 11].

Several experimental studies have indicated that the licofelone, a dual competitive inhibitor of cyclooxygenases COX-1 and COX-2 and 5-lipoxygenase (5-LOX), has analgesic, anti-inflammatory, anti-asthmatic and anti-platelet effects, with greater gastrointestinal safety than traditional non-steroidal anti-inflammatory drugs (NSAIDs); [12-15]. Clinical studies reported that licofelone was as effective as celecoxib, a COX-2-specific inhibitor, but had better gastrointestinal tolerability [12, 16]. We demonstrated that licofelone was more effective than celecoxib in suppressing colonic tumors in APC^{min} mice [17]. It is widely accepted that selectively blocking COX-2 will shift arachidonic acid metabolism towards the 5-LOX pathway, overproducing leukotrienes and leading to increased prothrombotic effects [14, 18, 19]. This might be a mechanism of action for licofelone's low gastric damage and anti-arthritic activity [20, 21]. Preclinical studies show that NSAIDs may inhibit lung cancer both *in vitro* and *in vivo*. However, these studies are yet to be translated to clinical practice.

From published data it is assumed that combination of NSAIDs and polyamine inhibitors due to their suppressive effects might lead to increased anti-carcinogenic results [22]. Further, combinations of these drugs could offer the potential of efficacy at much lower concentrations than would have been required if they were used independently. Most previous research was conducted *in vitro*, evaluating the effect of either DFMO or licofelone alone at high concentrations. To our knowledge, this is the first study evaluating the effect of a combination of DFMO and licofelone on progression from adenoma to adenocarcinoma in NNK-induced lung cancer in A/J mice.

Materials and methods

Chemicals, antibodies, and reagents

NNK (>99% purity) was synthesized and kindly provided by the laboratory of Dr. Shantu Amin (Department of Pharmacology, Penn State Hershey, PA). Sodium orthovandate, Triton X-100, EDTA, EGTA, Igepal CA-630 (I7771), and protease inhibitor cocktail (P8340) were purchased from Sigma Chemical Co. (St Louis, MO, USA). Sodium fluoride, β-glycerophosphate, and phenylmethanesulfonylfluoride were purchased from Alfa Aesar (MA, USA). Primary antibodies against p-p38, pAKT, and MMP-2 were obtained from Bioss Antibodies (Massachusetts, USA). Primary antibody against PCNA and anti-rabbit, -goat, and -mouse horseradish-peroxidase (HRP)-conjugated secondary antibodies were purchased from Santa Cruz Biotechnology (Santa Cruz, CA, USA). Antibodies against Cyclin D1 and NFκB were purchased from Cell Signaling Technology (Beverly, MA, USA). Histostain®-Plus 3rd Gen IHC Detection Kits were purchased from Life Technologies (NY, USA).

Animals, diet, and care

All animal experiments were performed in accordance with National Institute of Health (NIH) guidelines and the approval of the University of Oklahoma Health Sciences Center Institutional Animal Care and Use Committee. Six-week-old female A/J mice were obtained from Jackson Laboratory (Bar Harbor, ME). Mice were housed in ventilated cages under standardized conditions (21°C, 60% humidity, 12-h light/12-h dark cycle, 20 air changes per hour) in the pathogen-free University Rodent Barrier Facility. Semi-purified modified AIN-76A diet ingredients were purchased from Bioserv, Inc. (Frenchtown, NJ) and were stored at 4°C before preparation. Diets were prepared based on the modified American Institute of Nutrition (AIN)-76A diet as described earlier [23]. DFMO and licofelone were kindly supplied by the National Cancer Institute, Division of Cancer Prevention Repository (Bethesda, MD). Test agents were premixed with a small quantity of casein and were then blended into bulk diet using a Hobart Mixer. Both control and experimental diets were prepared weekly and stored in a cold room. Mice were allowed ad-libitum access to the diets and automated tap water purified by reverse osmosis; and checked rou-

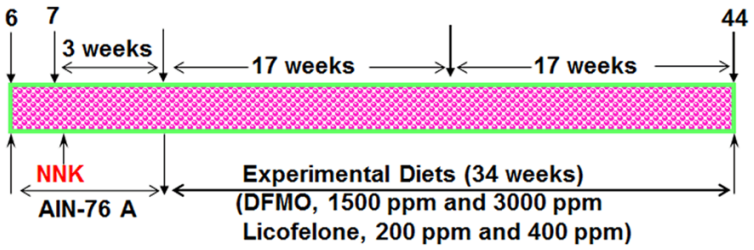

Figure 1. Experimental design for evaluating the chemopreventive effect of DFMO, licofelone, and the combination in NNK-induced lung cancer in the A/J mouse model. Six-week-old mice were injected intraperitoneally with NNK (10 μmol/mouse). Mice were maintained on AIN-76A diet for 3 weeks. Three weeks after NNK injection, mice were fed with control diet (AIN-76A) or experimental diets containing 1500 or 3000 ppm of DFMO, 200 or 400 ppm licofelone, or a low-dose combination of DFMO and licofelone. Treatment continued until the end of the study. At 17 weeks (10 mice/group) and at 34 weeks (15 mice/group) after NNK treatment excluding 3 weeks of wash out period after NNK treatment, mice were killed and lungs were harvested for evaluation of lung tumors. Detailed information is provided in the materials and methods section.

tinely for signs of weight loss, toxicity, or any abnormalities. Food cups were replenished with fresh diet twice weekly during experimental period.

Experimental bioassay

The experiment was designed to evaluate the effects of short-term (during the progression of adenomas/early adenocarcinomas) and long-term (adenoma to adenocarcinomas) exposure to DFMO and licofelone on NNK-induced lung carcinogenesis in A/J mice. The experimental design is summarized in **Figure 1**. Female A/J mice were randomly categorized by weight into control and experimental groups. At 8 weeks of age, the mice intended for carcinogen treatment received a single intraperitoneal dose of 10 μmol NNK. Three weeks after NNK injection, groups of mice (25/group) were fed control AIN-76A or experimental diets containing DFMO (1500 or 3000 ppm), licofelone (200 or 400 ppm), or a combination of DFMO (1500 ppm) and licofelone (200 ppm), until study termination. Mice were euthanized by CO_2 asphyxiation after 17 weeks (10 mice/group) or 34 weeks (15 mice/group) of exposure to the test agents. All mice were weighed once every two weeks until termination of the study. After euthanasia, lungs were lavaged, perfused, and either snap-frozen in liquid nitrogen for protein and mRNA analysis or fixed in phosphate-buffered formalin, transferred within 2 days to 70% alcohol, and evaluated under a dissecting microscope for the number of tumors and tumor size. Tumors on the lung surface were counted under a dissecting microscope by at least two experienced readers who were blinded to sample identifiers. Tumor diameters were measured using Fisher brand digital callipers.

Tumor histology

Fixed lung samples were embedded in paraffin, sectioned, and stained with hematoxylin and eosin (H&E). H & E-stained lung sections from three predetermined depths were evaluated in a blinded manner by a board-certified pathologist to obtain the number of adenomas and adenocarcinomas. Tumors were categorized according to the criteria of the Mouse Models of Human Cancers Consortium [24].

Protein immunoblotting

Lungs were frozen immediately in liquid nitrogen and stored at -80°C for further analysis. For marker analysis, tumors were excised from the lungs and total cell lysates were prepared using a previously described cell fractionation procedure [25]. Proteins were resolved on 8-12% SDS-PAGE, were transferred to a nitrocellulose membrane, and were probed with specific antibodies overnight at 4°C. The membranes were washed three times with Tris-buffered saline (TBS; pH 7.4) or phosphate-buffered saline (PBS; pH 7.4) for 15 min. Then, membranes were incubated with anti-rabbit or anti-goat or anti-mouse horseradish peroxidase-conjugated secondary antibody (1:5000, 2.5% skimmed milk in TTBS) and visualized using chemiluminescence reagent from Thermo Scientific (USA), followed by autoradiography. β-actin was used as the loading control. Densitometry of various analyte proteins and their respective loading controls from the same blot was performed using ImageJ 1.43 (NIH) software. Relative optical density was calculated by dividing the densitometry of analyte(s) protein with the respective loading control.

Immunohistochemical staining

For immunohistochemical (IHC) staining, normal and tumor tissues were fixed in 10% buffered formalin and expression was evaluated in adenocarcinomas by immunohistochemistry (IHC) as described in our previous paper [26]. Briefly, formalin-fixed, paraffin-embedded, 5-μm-thick tissue sections were mounted on white frosted, positive-charged (Denville Scientific, USA) glass slides. Sections were deparaffinised with xylene, rehydrated through a gradient series of alcohol, and washed in PBS. Antigen retrieval was carried out by heating sections in citrate buffer (10 mM, pH 6) for 30 minutes in a boiling water bath. Detection was conducted using a Histostain®-Plus 3rd Gen IHC Detection Kit (Life Technologies, USA). Endogenous peroxidase activity was quenched by incubating the sections with peroxidase quenching solution for 30 min in darkness. Nonspecific binding sites were blocked with blocking solution for 1 h. Sections were then incubated with specific antibodies overnight at 4°C. The next day, the slides were washed with PBS and incubated with biotinylated secondary antibody for 1 h in a humidified chamber. After three 5-minute washes, the slides were incubated with streptavidin-peroxidase conjugate. After rinsing with PBS, diaminobenzidine was employed as the chromogenic substrate. The slides were counterstained with Mayor's hematoxylin. For negative or isotype controls, the primary antibody was replaced with TBS or the respective antibody serum (used at the appropriate concentration). Slides were observed under an Olympus microscope IX71. Digital computer images were recorded with an Olympus DP70 camera.

Immunofluorescence staining

Formalin-fixed, paraffin-embedded, 5-μm-thick tissue sections were used to examine protein expression, as described elsewhere [27]. After deparaffinization, rehydration, antigen unmasking, and endogenous peroxidase activity blocking, sections were treated with freshly prepared 1% sodium borohydrate in distilled water for 30 min at room temperature. Sections were subsequently incubated with 1% bovine serum albumin (BSA) in PBS for 1 h to prevent nonspecific binding. After incubation with primary antibody, sections were incubated for 1 h with anti-rabbit or anti-goat Alexa Fluor® 488 (Life Technologies) secondary antibodies. Slides were washed three times for 10 min with PBST and were then incubated with 4', 6'-diamidino-2-phenylindole (DAPI; 100 ng/ml) for 20 min. The slides were mounted with SlowFade Gold antifade reagent (Life Technologies) with coverslips and were sealed with nail enamel. Slides were observed under an Olympus microscope IX71. Digital computer images were recorded with an Olympus DP70 camera.

Quantitative real-time PCR analysis

Total RNA from normal and tumor samples was extracted using TRizol reagent for total cellular RNA (Invitrogen, Grand Island, NY) per the manufacturer's instructions. Equal amounts of DNA-free RNA were used for reverse transcription (RT) reactions to make cDNA using an iScript cDNA synthesis kit (Bio-Rad) per the manufacturer's protocol. Real-time PCR was carried out in a 12-μl reaction volume containing 5 μl of diluted cDNA (50 ng) and FastStart Universal SYBR Green master (Roche) and primers (Invitrogen; Supplementary Table 1). All PCRs were performed in a Bio-Rad iCycler iQTM5 real-time PCR detection system. The fluorescence threshold values (Ct) were calculated. Relative mRNA levels were assessed by standardization to actin or GAPDH. Results are expressed as a relative fold difference in gene expression compared with control. Relative gene expression was calculated using the 2-ΔΔCT formula [28]. Specific primers for different genes were designed (see Supplementary Table 1). PCR conditions were as follows: denaturation at 94°C for 10 minutes, followed by 40 cycles at 95°C for 30 seconds, 60°C for 30 seconds, and 72°C for 45 seconds. All experiments were performed in triplicate.

Statistical analysis

Differences in body weights among groups were analyzed using analysis of variance. Adenoma and adenocarcinoma multiplicities (number of tumors/mouse) are expressed as means ± *SEM*. Protein expression and proliferative indices are expressed as means ± *SEM* and were analyzed by unpaired *t*-test with Welch's correction. Dose-response effects were analyzed by linear regression analysis. Differences were considered statistically significant at $p < 0.05$. All statistical analysis was performed using Graphpad Prism 6.0.

Results

General observations

Dose selection was based on previously published toxicity studies. DFMO doses of up to ~5000 ppm and licofelone doses of up to ~600 ppm were tolerated in rodent models when administered with AIN-76A diet for 6 weeks [29]. In the present study, we applied 30% (1500 ppm) and 60% (3000 ppm) of the maximum tolerated dose (MTD) of DFMO and 30% (200 ppm) and 60% (400 ppm) of the MTD of licofelone to assess chemopreventive efficacy. We also administered a low-dose combination of 1500 ppm DFMO and 200 ppm licofelone to evaluate the efficacy of this combination. No significant changes in body weight or any other histologic toxicity in major organ sites were observed for either drug at any dose or time course (data not shown). The drugs did not induce any overt toxicities when administered through diet.

The combination of DFMO and licofelone significantly inhibits lung adenocarcinoma and delays the progression of adenoma to adenocarcinoma

NNK-treated mice fed on control diet developed 100% tumor incidence at 17 or 34 weeks (excluding wash-out period of 3 weeks after the carcinogen treatment, **Figure 2A** and **2B**). **Figure 2** shows the effects of both drugs and the combination on lung tumors, lung adenoma, and lung adenocarcinoma multiplicities at 17 and 34 weeks after treatment. Control-diet-fed mice that were killed at 17 weeks formed an average of 15.2 ± 1.29 lung tumors, while those killed at 34 weeks formed an average of 18.4 ± 1.4 lung tumors (**Figure 2A** and **2B**). Administration of 1500 ppm and 3000 ppm of DFMO significantly suppressed lung tumor formation by 25% ($p < 0.0001$) and 32% ($p < 0.001$) at 17 weeks post-administration and by 30% ($p = 0.0012$) and 44% ($p < 0.0001$) at 34 weeks post-administration (**Figure 2A** and **2B**). Treatment with 200 ppm and 400 ppm of licofelone significantly suppressed lung tumor formation by 17% ($p < 0.0001$) and 30% ($p < 0.0001$) at 17 weeks post-treatment and 32% ($p = 0.0008$) and 48% ($p < 0.0001$) at 34 weeks post-treatment (**Figure 2A** and **2B**). The low-dose combination of DFMO and licofelone significantly suppressed lung tumor formation by 51% ($p < 0.0001$) at 17 weeks post-treatment and 60% ($p < 0.0001$) at 34 weeks post-treatment (**Figure 2A** and **2B**).

Figure 2G displays representative H&E staining of lung tumors from mice fed with control diet, DFMO, licofelone, or the combination. Tumors were classified as adenoma or adenocarcinoma, as described earlier [24]. Adenocarcinomas in control-diet-fed mice had varying degrees of differentiation and were characterized as the complete loss of normal alveolar architecture compared with adenocarcinomas seen in mice fed with DFMO, licofelone, or the combination (**Figure 2G**). Our observations suggest that a low-dose combination of DFMO and licofelone delays the adenoma-to-adenocarcinoma progression. We observed a reduced amount of cytoplasm and a small degree of pleomorphism without loss of alveolar architecture, thus retaining the adenoma structure in combination-treated mice (**Figure 2G**) at 34 weeks, compared with controls and mice treated with either drug alone.

Further histopathologic analysis showed that control-diet-fed mice had 9.4 ± 0.7 (means ± *SEM*) adenomas and 5.8 ± 0.5 lung adenocarcinomas, reflecting 61.8% of adenomas and 38.2% of adenocarcinomas, at 17 weeks post diet treatment excluding 3 weeks of wash out period after NNK treatment (**Figure 2C** and **2E**). Control-diet-fed mice had only 2.2 ± 0.2 adenomas (11.9%) and 16.2 ± 0.7 adenocarcinomas (88.1%) at 34 weeks post diet treatment excluding 3 weeks of wash out period after NNK treatment weeks, reflecting a significant increase in the progression of adenomas to adenocarcinomas (**Figure 2D** and **2F**). Administration of 1500 ppm and 3000 ppm of DFMO significantly suppressed NNK-induced lung adenoma by 23% ($p < 0.001$) and 42% ($p < 0.0001$) and suppressed lung adenocarcinoma by 27% ($p < 0.01$) and 44% ($p = 0.0002$), respectively, at 17 weeks (**Figure 2C** and **2E**). However, at 34 weeks, the suppression was 13% (not significant) and 31% ($p < 0.002$) in lung adenoma and 33% ($p < 0.0001$) and 46% ($p < 0.0001$) in lung adenocarcinoma (**Figure 2D** and **2F**). At 17 weeks, 200 ppm and 400 ppm of licofelone significantly suppressed NNK-induced lung adenoma by 28% ($p < 0.003$) and 38% ($p < 0.0004$) and lung adenocarcinoma by 31% ($p < 0.005$) and 37% ($p < 0.0001$), respectively (**Figure 2C** and **2E**). However, at 34

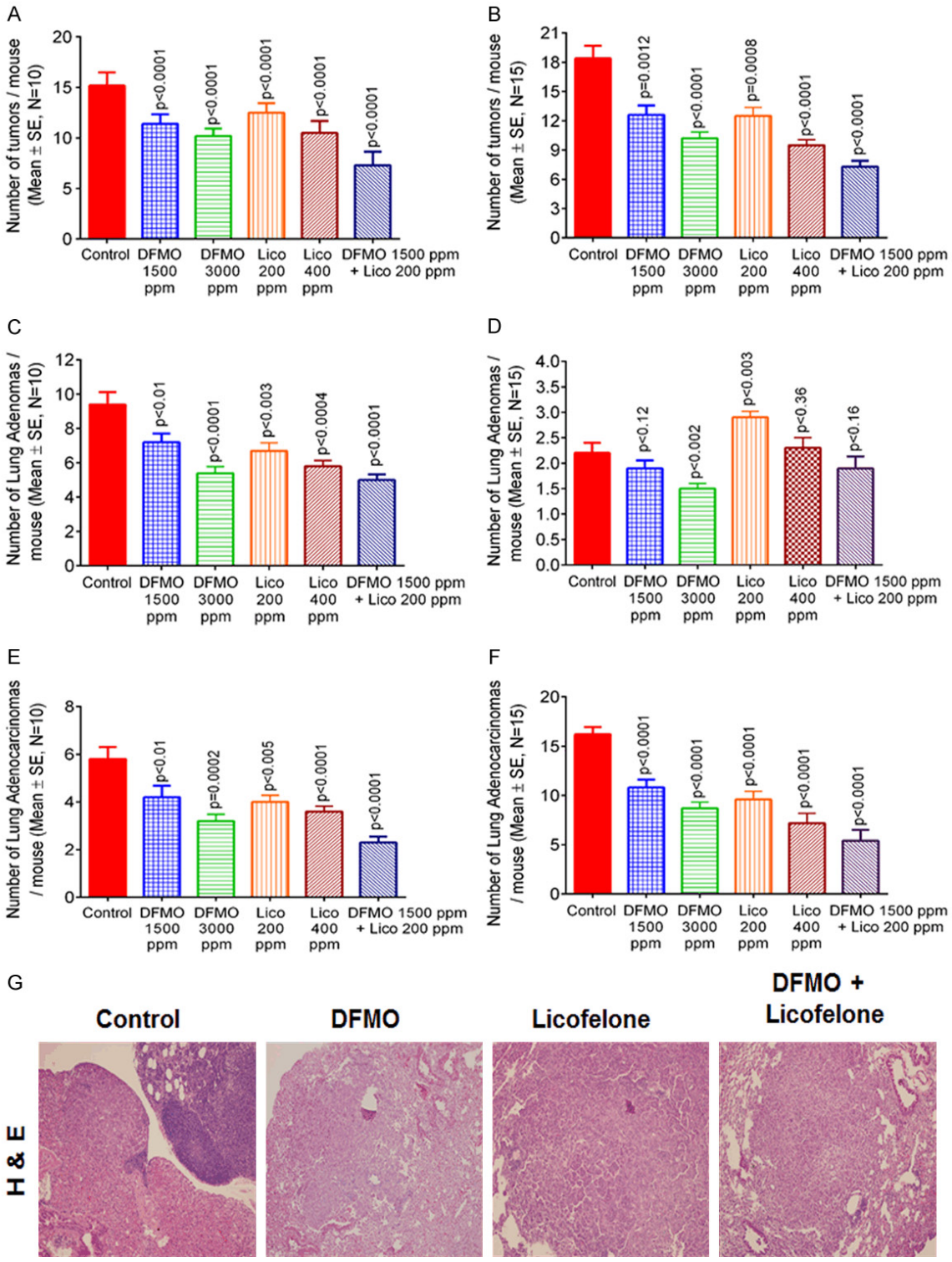

Figure 2. Effect of dietary feeding of DFMO, licofelone, and the combination on NNK-induced lung tumor growth in A/J mice. A. Lung tumors from different groups at the 17-week post diet treatment stage. B. Lung tumors from different groups at the 34-week post diet treatment stage. Effect of DFMO, licofelone, and the combination on NNK-induced lung adenoma in A/J mice. C. Lung adenoma from different groups at the 17-week post diet treatment stage. D. Lung adenoma from different groups at the 34-week post diet treatment stage. Values are means ± *SE* with *N* = 10. Effect of DFMO, licofelone, and the combination on NNK-induced lung adenocarcinoma in A/J mice. E. Lung adenocarcinoma from different groups at the 17-week post diet treatment stage. F. Lung adenocarcinoma

from different groups at the 34-week post diet treatment stage. Values are means ± *SE* with *N* = 15. Differences between control and treatment groups were analyzed by one-tailed *t*-test with Welch correction and 95% confidence interval. G. Representative photomicrograph of hematoxylin and eosin (H&E) staining of lung tumor sections from mice in different experimental groups.

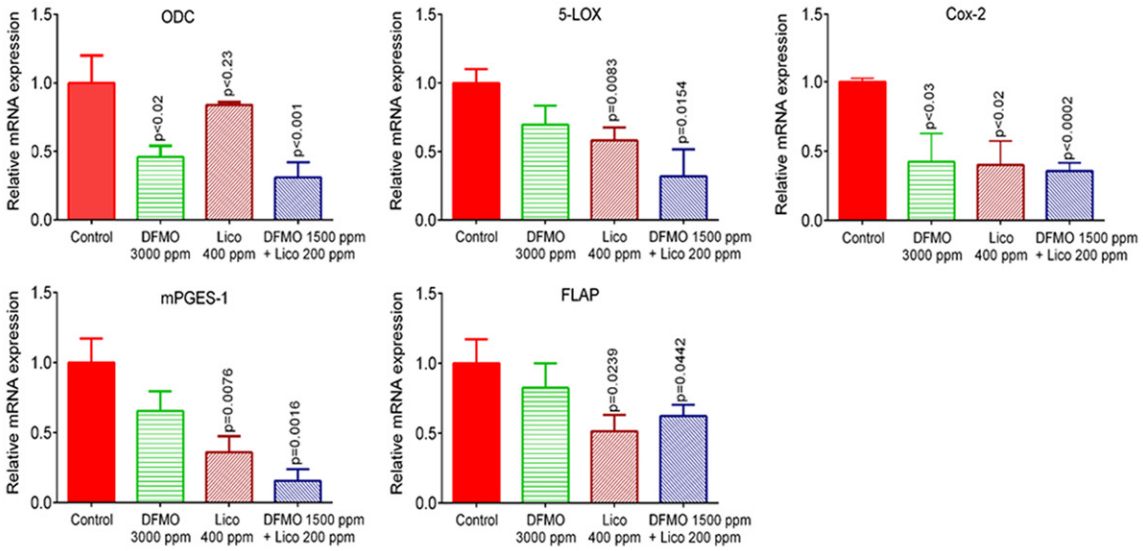

Figure 3. Effect of DFMO, licofelone, and the combination on ODC, 5-Lox, Cox-2, mPGES-1, and FLAP mRNA expression in NNK-induced lung tumor from mice in different treatment groups. Relative mRNA expression of ODC, 5-Lox, Cox-2, mPGES-1, and FLAP in RNA samples from different treatment groups as analyzed by real-time PCR and normalized to β-actin. Significance of differences between control and treatment groups was analyzed by one-tailed *t*-test with Welch correction and 95% confidence interval. Data with means ± *SE*. $p \leq 0.05$ was considered statistically significant.

weeks post-treatment, mice treated with either dose of licofelone had slightly more lung adenomas (31% and 4%, not significant) and significantly fewer lung adenocarcinomas (40% and 55%, $p < 0.0001$), reflecting some delay in the progression from adenoma to adenocarcinoma (**Figure 2D** and **2F**). The combination treatment significantly suppressed lung adenoma by 46% ($p < 0.0001$) and lung adenocarcinoma by 60% ($p < 0.0001$) at 17 weeks post-treatment (**Figure 2C** and **2E**). At 34 weeks post-treatment, the suppression was 13% in lung adenoma and 64% ($p < 0.0001$) in lung adenocarcinoma, suggesting that the low-dose combination of DFMO and licofelone was more effective than were higher doses of DFMO or licofelone alone (**Figure 2D** and **2F**).

A combination of DFMO and licofelone inhibits the expression of COX-2, 5-LOX, mPGES1, and FLAP

We used real-time PCR and immunohistochemistry to examine mRNA and protein levels of pro-inflammatory enzymes COX-2 and 5-LOX in lung tumors. DFMO was less effective in inhibiting the expression of COX-2 and 5-LOX at mRNA and protein levels compared to licofelone and the combined treatment (**Figures 3** and **4**). We observed a significant reduction in mRNA expression of COX-2, 5-LOX, mPGES1, and FLAP in tumors from mice fed with licofelone and the combined treatment compared with tumors from mice fed with control diet (**Figure 3**). Only COX-2 mRNA expression was significantly inhibited by DFMO (**Figure 3**). Further, the low-dose combination of DFMO and licofelone was found to be more effective in decreasing the immunohistochemical staining of COX-2 and 5-LOX than were controls and either drug alone (**Figure 4**).

A low-dose combination of DFMO and licofelone modulates the ODC signaling in NNK-induced lung tumors

ODC catalyzes the first step in the polyamine biosynthetic pathway, the decarboxylation of

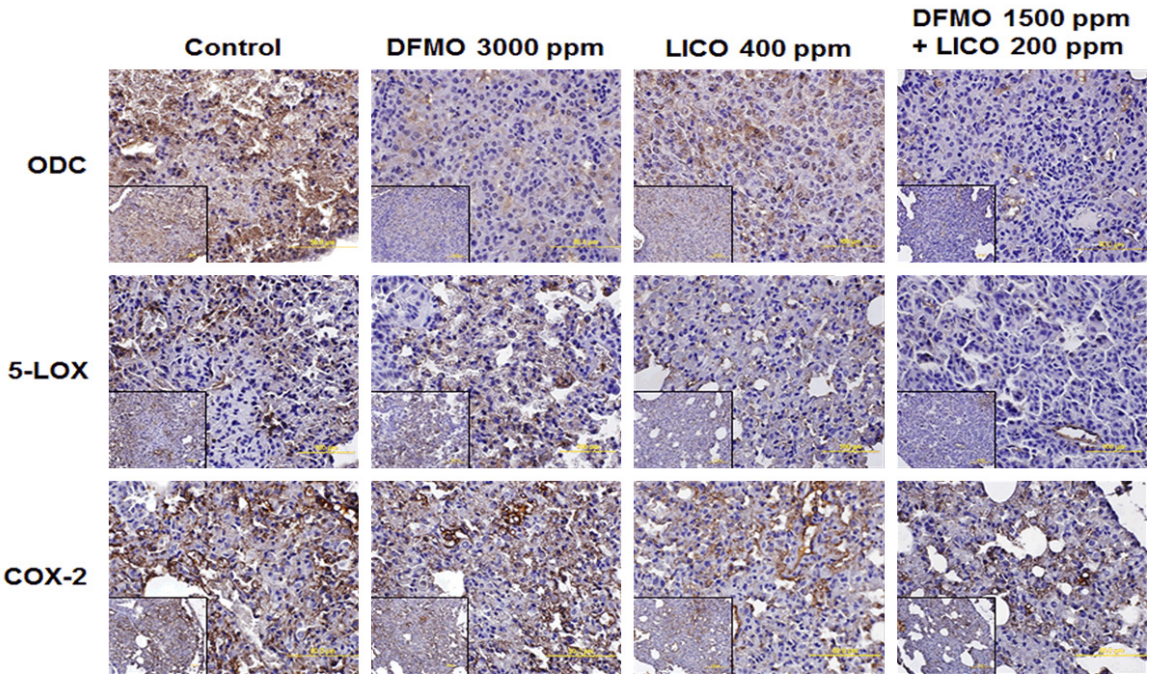

Figure 4. Effect of DFMO, licofelone, and the combination on ODC, 5-Lox, and Cox-2 expression in NNK-induced lung tumor sections from mice in different treatment groups. Representative photomicrographs showing immunohistochemical detection of ODC, 5-Lox, and Cox-2 (magnification ×600; inset shows 400× magnification).

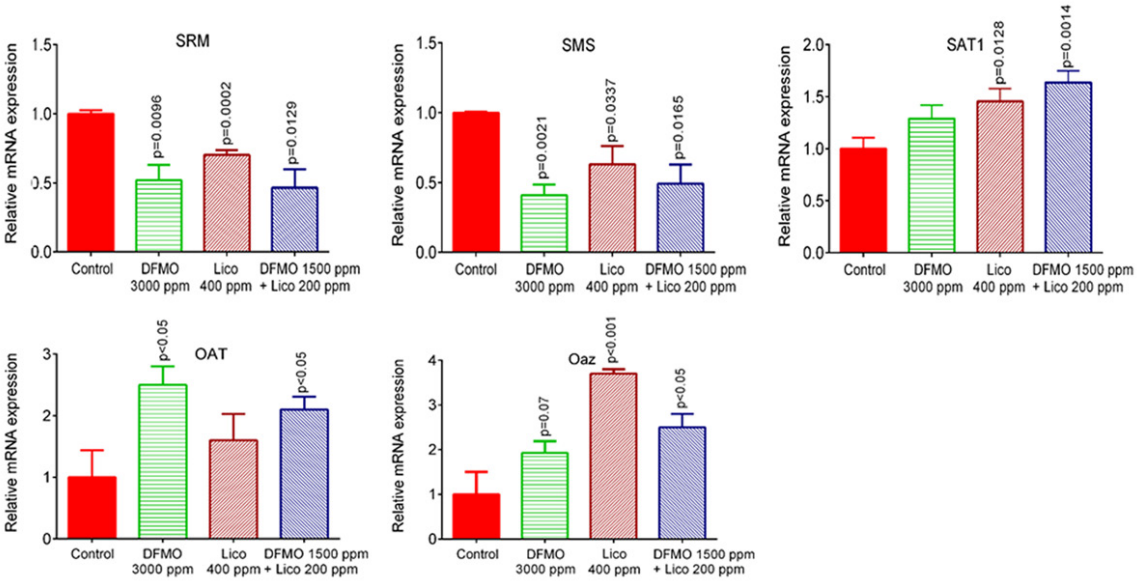

Figure 5. Effect of DFMO, licofelone, and the combination on the polyamine synthesis pathway. Relative mRNA expression of spermidine synthase (SRM), spermine synthase (SMS), spermidine N(1)-acetyl transferase (SAT), ornithine amino transferase (Oat), and antizyme (Oaz) in RNA samples from different treatment groups as analyzed by real-time PCR and normalized to β-actin. Differences between control and treatment groups were analyzed by one-tailed *t*-test with Welch correction and 95% confidence interval. Data represent means ± *SE*. $p \leq 0.05$ was considered statistically significant.

ornithine to putrescine. ODC is modulated by other signaling molecules of the polyamine pathway, including Oat, Oaz, SRM, SMS, and SAT1; its activation can lead to tumor promo-

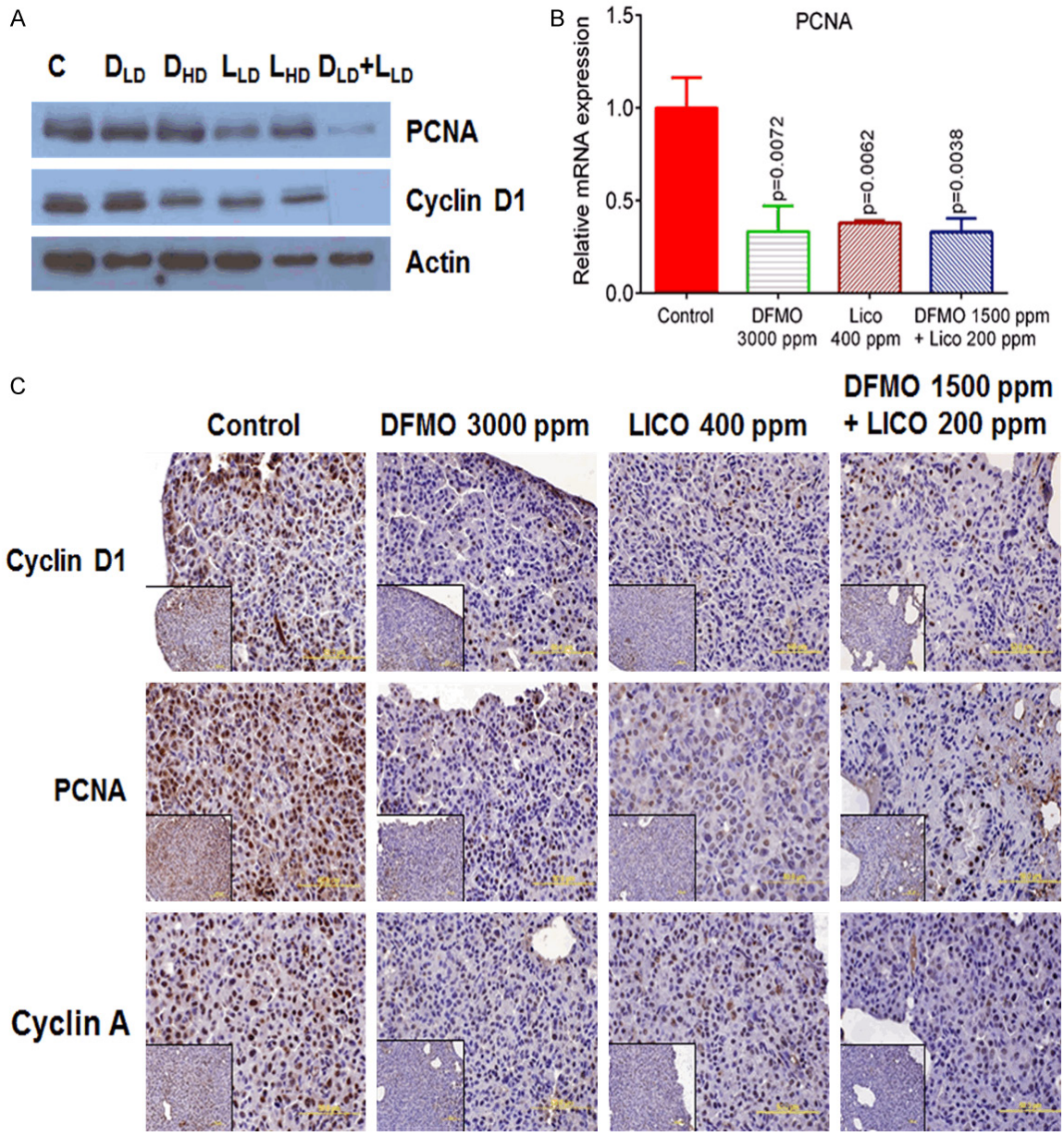

Figure 6. Effect of DFMO, licofelone, and the combination on cell proliferation markers in NNK-induced lung tumors from mice in different treatment groups. A. Representative western blot of PCNA and Cyclin D1 measured in total cell protein of tumor. B. Relative mRNA expression of PCNA in RNA samples from different treatment groups as analyzed by real-time PCR and normalized to β-actin. C. Representative photomicrographs showing immunohistochemical detection of PCNA, Cyclin D1, and Cyclin A (magnification ×600; inset shows 400× magnification). Differences between control and treatment groups were analyzed by one-tailed *t*-test with Welch correction and 95% confidence interval. Data with means ± *SE*. $p \leq 0.05$ was considered statistically significant.

tion and progression. The expression of ODC and its related signaling molecules was first analyzed in normal lung and tumor tissues using real-time quantitative PCR assays (qPCR). We observed that mRNA levels of ODC, SRM, and SMS significantly increased in lung tumor tissue compared with normal tissue. The ODC-inhibitory enzyme Oaz, the polyamine-degrading enzyme SAT1, and Oat were significantly downregulated in lung tumor tissue compared with normal lung (Supplementary Figure 1).

Further, ODC pathway signaling molecules were measured using IHC and qPCR in lung tumor

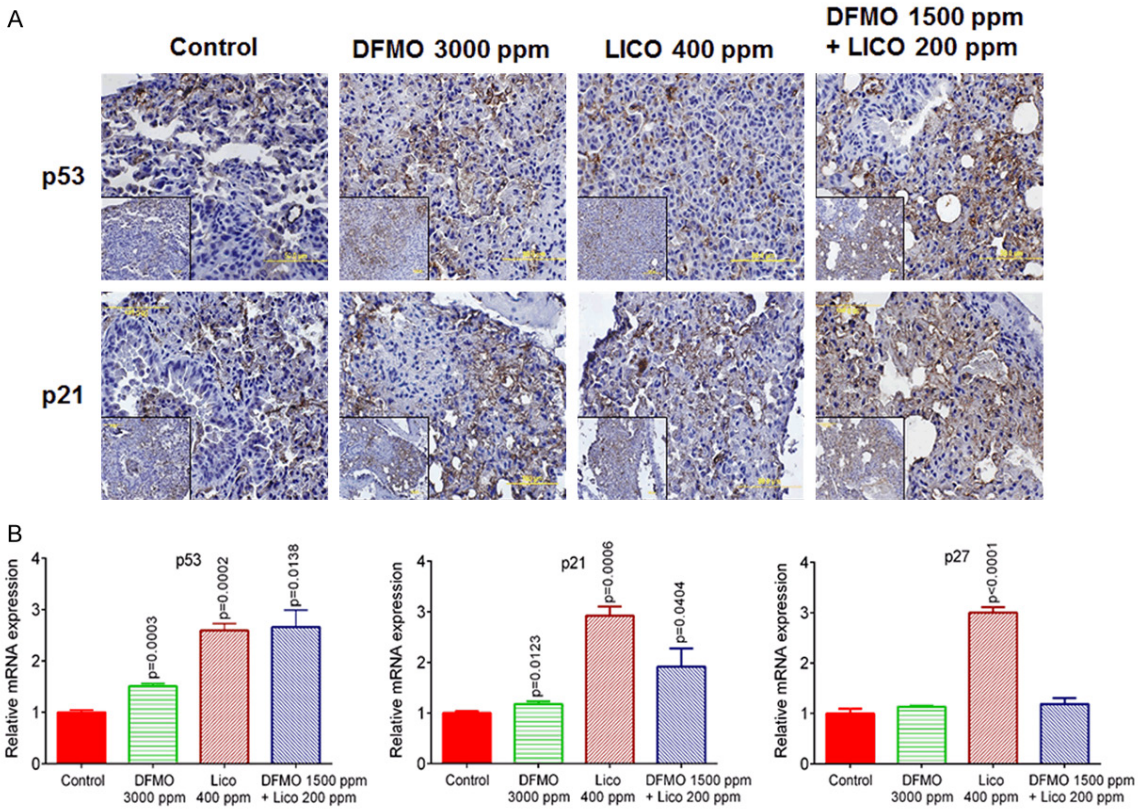

Figure 7. Effect of DFMO, licofelone, and the combination on p53, p21, Bax, and p27. A. Representative photomicrographs showing immunohistochemical detection of p53 and p21 (magnification ×600; inset shows 400× magnification). B. Relative mRNA expression of p53, p21, Bax, and p27 in RNA samples from different treatment groups as analyzed by real-time PCR and normalized to β-actin. Differences between control and treatment groups were analyzed by one-tailed *t*-test with Welch correction and 95% confidence interval. Data represent means ± *SE*. $p \leq 0.05$ was considered statistically significant.

tissues. Markedly reduced mRNA and protein expression of ODC was observed in combination-treated mice compared with single-drug-treated and control-diet-fed mice (**Figures 3** and **4**). mRNA expression levels of SRM and SMS were reduced and mRNA expression levels of Oat, Oaz, and SAT1 were increased in lung tumors from combination-treated mice compared with control-diet-fed mice (**Figure 5**).

A low-dose combination of DFMO and licofelone inhibits tumor cell proliferation and induces p21, p27, and p53

We used immunoblotting/IHC and qPCR techniques to examine protein and mRNA expression of Cyclin D1, PCNA, and Cyclin A1 in mouse lung tumor tissues. The low-dose combination of DFMO and licofelone significantly decreased PCNA and Cyclin D1 protein expression compared with either drug alone or controls (**Figure 6A** and **6C**). The combination was more effective in decreasing the intensity of IHC staining of PCNA and Cyclin D1 than was either drug alone. We also observed similar alterations in mRNA levels of PCNA in tissues obtained from mice fed with the low-dose combination (**Figure 6B**). Further, levels of Cyclin A protein, a cell cycle regulator, were inhibited in lung tumors from mice receiving the low-dose combination compared with tumors from mice fed control diet (**Figure 6C**).

Further, we measured p53, p21, and p27 protein/mRNA levels and observed a significant increase in their expression accompanying the low-dose combination of DFMO and licofelone (**Figure 7**). Taken together, these results suggest that the low-dose combination inhibits tumor progression, which is associated with reduced tumor cell proliferation. These findings are consistent with our *in vivo* tumor inhibition findings.

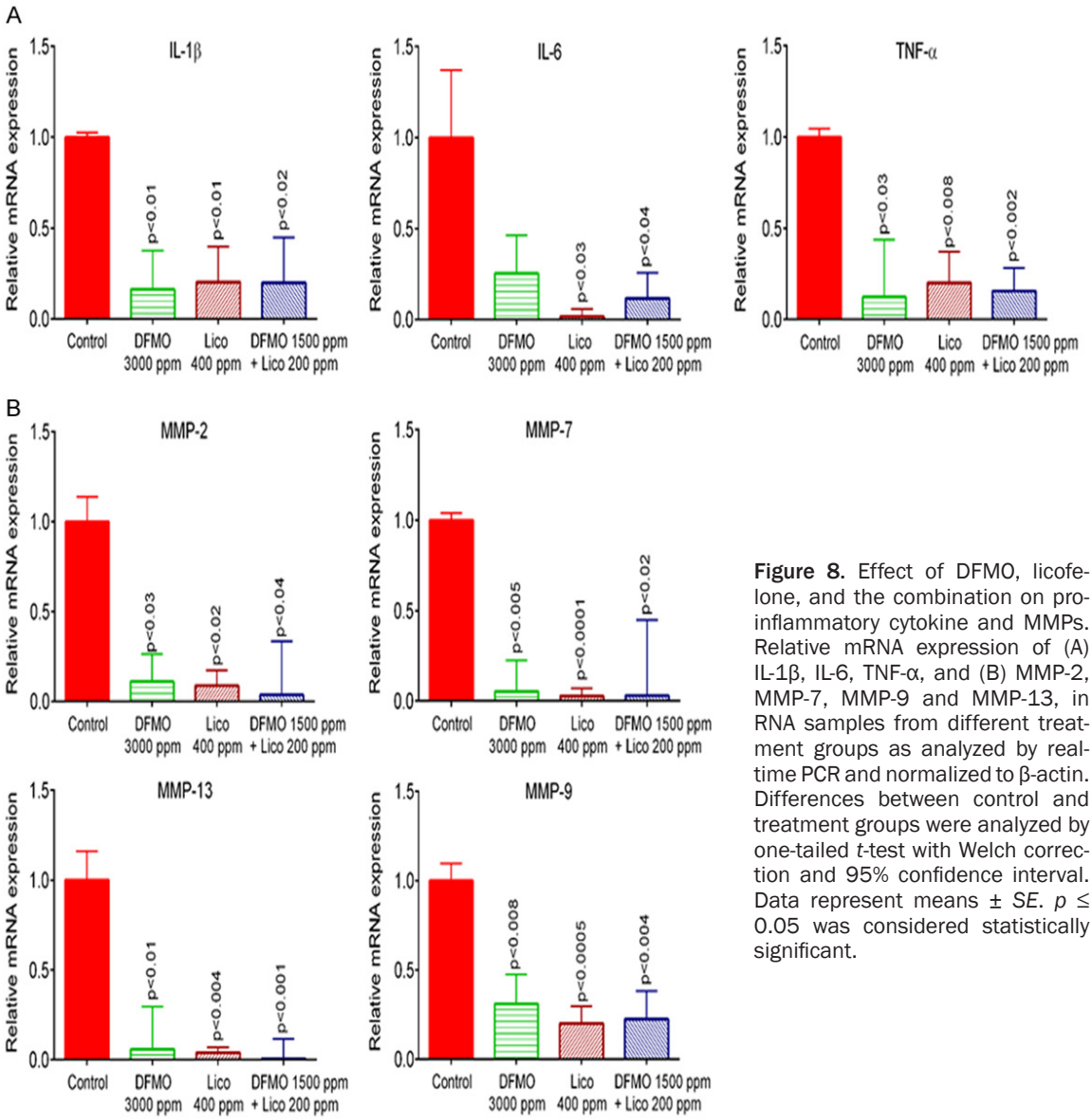

Figure 8. Effect of DFMO, licofelone, and the combination on pro-inflammatory cytokine and MMPs. Relative mRNA expression of (A) IL-1β, IL-6, TNF-α, and (B) MMP-2, MMP-7, MMP-9 and MMP-13, in RNA samples from different treatment groups as analyzed by real-time PCR and normalized to β-actin. Differences between control and treatment groups were analyzed by one-tailed *t*-test with Welch correction and 95% confidence interval. Data represent means ± *SE*. $p \leq 0.05$ was considered statistically significant.

Dietary administration of DFMO, licofelone, and the low-dose combination inhibits inflammatory cytokines and matrix metalloproteinases

Inflammation within the tumor microenvironment is correlated with increased invasiveness and poor prognosis. The cytokines interleukin-1 beta (IL-1β), interleukin-6 (IL-6), and tumor necrosis factor alpha (TNF-α) are critical mediators of the inflammatory response. Therefore, we evaluated the mRNA expression of IL-1β, IL-6, and TNF-α in control and drug-treated lung tumor tissues. Mice fed with DFMO, licofelone, and a low-dose combination displayed reduced mRNA levels of IL-1β, IL-6, and TNF-α (**Figure 8A**).

Matrix metalloproteinases (MMPs) are involved in tissue remodelling and disease processes, including cancer [30]. In addition to modifying extracellular matrix proteins, MMPs are intimately involved in the regulation of the activities of cytokines and cytokine receptors. Further, the control and drug-treated lung tumor tissues were analyzed for mRNA expression of MMP-2, MMP-7, MMP-9, and MMP-13. Compared with controls, mice fed with DFMO, licofelone, and the low-dose combination had lower mRNA levels of MMP-2, MMP-7, MMP-9,

and MMP-13, as measured by real-time PCR (**Figure 8B**). Further, we used IHC/IF to compare MMP-9 levels in control and drug-treated mice. Our results showed that MMP-9 was inhibited by the low-dose combination of DFMO and licofelone, compared with controls (Supplementary Figure 2).

Discussion

Increased polyamine synthesis and inflammation, which are risk factors for cancer progression in humans, have long been associated with intraepithelial neoplasia. Targeting polyamine metabolism with polyamine synthesis inhibitors or catabolism activators and inflammation with NSAIDs has been studied in many malignancies, including lung, colon, prostate, bladder, and skin cancers [4, 13, 14, 31]. Recent literature provides a basis for developing a combined treatment of chemopreventive and chemotherapeutic agents. In recent studies, inhibiting multiple molecular targets by administering a combination of their specific inhibitors was shown to block the pathogenesis of highly invasive and metastatic cancers more effectively than did single-agent-based therapeutic strategies [29, 32]. Inflammatory eicosanoids and leukotrienes derived from COX-2 and 5-LOX pathway positively influence lung tumor growth. Prominent over-expression of ODC, COX-2, and 5-LOX enzymes activity and polyamines has been associated with proliferation and progression of lung cancer; expression of these proteins is correlated with tumor grade and invasion in some reports [13, 14, 17, 22, 33]. It has been widely accepted that selectively blocking COX-2 will shift arachidonic acid metabolism towards the 5-LOX pathway, overproducing leukotrienes and leading to increased prothrombotic effects [14, 18, 19]. Targeting both tumor inflammatory molecules and polyamines synthesis may provide additive/synergistic antitumor effects. Hence, we chose licofelone as an anti-inflammatory agent due to its ability to simultaneously inhibit COX and 5-LOX (16) and to limit undesirable cardiovascular and gastrointestinal side effects, and selected DFMO as the ODC inhibitor to study their individual and combined effects on lung tumor progression.

The total number of tumors decreased by >51% and adenocarcinomas decreased by >60% in mice receiving treatment with the low-dose combination of DFMO and licofelone for 17 or 34 weeks. These reductions were even greater than those observed with administration of higher doses of DFMO (>32% in total tumors, >44% in adenocarcinomas) and licofelone (>30% in total tumors, >37% in adenocarcinomas) alone. These results are consistent with studies using individual DFMO or licofelone in different organ-site cancers [4, 13, 14]. Our findings suggest that a low-dose combination of DFMO and licofelone significantly inhibits the number of lung tumors, slowing the progression of NNK-induced lung lesions to adenoma and then to adenocarcinoma. There are limited reports on the evaluation of COX-2 inhibitors, and no reports on dual COX/5-LOX inhibitors used in combination with ODC inhibitors against an NNK-induced mouse model of lung cancer. This is the first report on the chemopreventive effects of DFMO and licofelone on NNK-induced lung carcinogenesis in the A/J mouse strain.

We observed that lung tumors from NNK-induced A/J mice have elevated levels of ODC, COX-2, and 5-LOX, compared to normal tissue. Mice fed with the low-dose combination of DFMO and licofelone showed reduced expression of ODC, COX-2, and 5-LOX at protein and mRNA levels compared with mice receiving higher doses of either drug alone. This finding suggests that the inflammation and polyamine pathways play significant roles in lung tumor progression. Thus, a combined treatment that inhibits polyamines and COX-2 and LOX-5 is a valid approach. mPGES-1 and FLAP share significant sequence homology and protein structure, having pathological roles in inflammatory diseases, and require glutathione (GSH) as an essential cofactor for their activity [34]. Our results showed that the low-dose combination of DFMO and licofelone also decreased the mRNA levels of mPGES-1 and FLAP, thereby reducing the inflammation.

We examined the mRNA expression of 1) Oaz, an enzyme that regulates polyamine synthesis by binding and inhibiting ODC, 2) Oat, an enzyme that regulates the conversion of ornithine into proline *via* Glutamate-γ-semialdehyde, and 3) SAT1, a rate-limiting enzyme in the catabolic pathway of polyamine metabolism. These constituents of the ODC pathway were significantly lower in lung tumors than in normal lung tissues. Inhibition of ODC and modulation of several components of polyamine biosynthesis

were observed in lung tumors from mice fed with high doses of DFMO or licofelone alone. However, the low-dose combination of DFMO and licofelone led to a significant reduction in ODC, SRM, and SMS expression, and increased Oaz and Oat expression. These results are consistent with previous reports on polyamine biosynthesis in various cancers [14, 35] and in lung cancer progression [22].

Uncontrolled proliferation is a hallmark of cellular transformation and is accompanied by the deregulation of proteins involved in the control of cell cycle checkpoints. Inflammation and polyamines are known to play a role in the transition of the cell cycle from G2/M to the G1 phase; this process is delayed by a reduction in polyamine levels [36]. Our results showed reduced PCNA, Cyclin A and Cyclin D1, and significantly increased p53 and p21, in mice fed with the low-dose combination of DFMO and licofelone compared with mice fed with a high dose of either drug alone. These findings are consistent with our earlier reports demonstrating that PCNA-positive cells and Cyclin D1 decreased after treatment with either DFMO or licofelone in colon, bladder, and pancreatic cancer [4, 6, 13, 14].

Transcription of Cyclin A is indirectly regulated by the tumor suppressor protein p53. Activated p53 turns on several downstream pathways, including p21, leading to cell cycle arrest [37]. Our study also showed reduced Cyclin A and increased p53 and p21 in mice-fed with a low-dose combination of DFMO and licofelone. This finding was consistent with those of other researchers [4, 13, 14, 38].

TNF is one of the main mediators of acute and chronic inflammation: it can induce IL1β and IL6 expression [39]. High circulating levels of IL-6 were reported to be associated with poor prognosis in patients with lung cancer [40]. However, IL-1β is a pluripotent cytokine that promotes angiogenesis, tumor growth, and metastasis in experimental models; its presence in some human cancers is associated with aggressive tumor biology [41]. Our results indicate that high doses of DFMO and licofelone alone and a low-dose combination of the two drugs significantly block the expression of IL-1β, IL-6, and TNF-α in NNK-induced lung tumors in A/J mice, as reported in earlier *in vitro* and *in vivo* studies [42].

Further, we observed the role of interleukins (ILs) in regulation of MMP. As in many immunological responses, cell type-specific activation of various MMPs is principally mediated by ILs, other cytokines, eicosanoids like prostaglandin E (PGE) and leukotriene B (LTB), and other inflammatory mediators [43]. Boileau et al. showed that licofelone dose dependently inhibited the IL-1β stimulated production and expression of MMP-13 [44]. Our results suggest that the low-dose combination of DFMO and licofelone inhibits the expression of MMP-2, -7, -9, and -13 in lung tumors, as was also reported in *in vitro* and *in vivo* studies and research into human cancers of different origins [5, 44, 45].

In summary, this is the first report of the chemopreventive effects of a low-dose combination of DFMO and licofelone on NNK-induced lung carcinogenesis in the A/J mouse strain. Both agents were more effective at inhibiting adenocarcinoma multiplicity and reducing the total number of tumors when mice were treated for 17 and 34 weeks. Our observations suggest that inflammation and polyamine synthesis modulating agents delay the adenoma to adenocarcinoma progression. Approximately 60% inhibition of adenomas and adenocarcinomas was observed in the mice fed with the low-dose combination of DFMO and licofelone, compared with the mice fed with high doses of either drug alone or control diet.

Acknowledgements

The authors thank the University of Oklahoma Health Sciences Center Rodent Barrier Facility and Ms. Kathy Kyler for valuable suggestions and editorial help. This study was funded by NCI-N01-CN-53300.

Disclosure of conflict of interest

None.

Abbreviations

Arg1, arginase; BSA, bovine serum albumin; HRP, horseradish peroxidase; IHC, immunohistochemical; Oat, ornithine amino transferase; Oaz, ornithine decarboxylase antizyme; PBS, phosphate-buffered saline; PVDF, polyvinylidene difluoride; qPCR, quantitative real-time; SAT, spermidine N(1)-acetyl transferase; SDS-PAGE, sodium dodecyl sulfate polyacrylamide

gel electrophoresis; SMS, spermine synthase; SRM, spermidine synthase; TBS, tris-buffered saline; TBST, TBS containing 0.1% Tween-20.

Address correspondence to: Dr. Chinthalapally V Rao, Center for Cancer Prevention and Drug Development, Hematology-Oncology Section, Department of Medicine, Stephenson Cancer Center, University of Oklahoma Health Sciences Center, 975 NE 10th Street, BRC West, Room 1203, Oklahoma City, OK 73104, USA. Fax: 405-271-3225; E-mail: cv-rao@ouhsc.edu

References

[1] Siegel RL, Miller KD and Jemal A. Cancer statistics, 2015. CA Cancer J Clin 2015; 65: 5-29.

[2] Lynch TJ, Adjei AA, Bunn PA Jr, Eisen TG, Engelman J, Goss GD, Haber DA, Heymach JV, Janne PA, Johnson BE, Johnson DH, Lilenbaum RC, Meyerson M, Sandler AB, Sequist LV, Settleman J, Wong KK and Hart CS. Summary statement: novel agents in the treatment of lung cancer: advances in epidermal growth factor receptor-targeted agents. Clin Cancer Res 2006; 12: 4365s-4371s.

[3] Hecht SS, Kassie F and Hatsukami DK. Chemoprevention of lung carcinogenesis in addicted smokers and ex-smokers. Nat Rev Cancer 2009; 9: 476-488.

[4] Mohammed A, Janakiram NB, Madka V, Ritchie RL, Brewer M, Biddick L, Patlolla JM, Sadeghi M, Lightfoot S, Steele VE and Rao CV. Eflornithine (DFMO) prevents progression of pancreatic cancer by modulating ornithine decarboxylase signaling. Cancer Prev Res (Phila) 2014; 7: 1198-1209.

[5] Mohammed A, Janakiram NB, Pant S and Rao CV. Molecular Targeted Intervention for Pancreatic Cancer. Cancers (Basel) 2015; 7: 1499-1542.

[6] Meyskens FL Jr, McLaren CE, Pelot D, Fujikawa-Brooks S, Carpenter PM, Hawk E, Kelloff G, Lawson MJ, Kidao J, McCracken J, Albers CG, Ahnen DJ, Turgeon DK, Goldschmid S, Lance P, Hagedorn CH, Gillen DL and Gerner EW. Difluoromethylornithine plus sulindac for the prevention of sporadic colorectal adenomas: a randomized placebo-controlled, double-blind trial. Cancer Prev Res (Phila) 2008; 1: 32-38.

[7] Simoneau AR, Gerner EW, Nagle R, Ziogas A, Fujikawa-Brooks S, Yerushalmi H, Ahlering TE, Lieberman R, McLaren CE, Anton-Culver H and Meyskens FL Jr. The effect of difluoromethylornithine on decreasing prostate size and polyamines in men: results of a year-long phase IIb randomized placebo-controlled chemoprevention trial. Cancer Epidemiol Biomarkers Prev 2008; 17: 292-299.

[8] Weiss TS, Bernhardt G, Buschauer A, Thasler WE, Dolgner D, Zirngibl H and Jauch KW. Polyamine levels of human colorectal adenocarcinomas are correlated with tumor stage and grade. Int J Colorectal Dis 2002; 17: 381-387.

[9] Hu HY, Liu XX, Jiang CY, Lu Y, Liu SL, Bian JF, Wang XM, Geng Z, Zhang Y and Zhang B. Ornithine decarboxylase gene is overexpressed in colorectal carcinoma. World J Gastroenterol 2005; 11: 2244-2248.

[10] Carlisle DL, Devereux WL, Hacker A, Woster PM and Casero RA Jr. Growth status significantly affects the response of human lung cancer cells to antitumor polyamine-analogue exposure. Clin Cancer Res 2002; 8: 2684-2689.

[11] Tian H, Li L, Liu XX and Zhang Y. Antitumor effect of antisense ornithine decarboxylase adenovirus on human lung cancer cells. Acta Biochim Biophys Sin (Shanghai) 2006; 38: 410-416.

[12] Payandemehr B, Khoshneviszadeh M, Varastehmoradi B, Gholizadeh R, Bahremand T, Attar H, Bahremand A and Dehpour AR. A COX/5-LOX Inhibitor Licofelone Revealed Anticonvulsant Properties Through iNOS Diminution in Mice. Neurochem Res 2015; 40: 1819-1828.

[13] Madka V, Mohammed A, Li Q, Zhang Y, Patlolla JM, Biddick L, Lightfoot S, Wu XR, Steele V, Kopelovich L and Rao CV. Chemoprevention of urothelial cell carcinoma growth and invasion by the dual COX-LOX inhibitor licofelone in UPII-SV40T transgenic mice. Cancer Prev Res (Phila) 2014; 7: 708-716.

[14] Mohammed A, Janakiram NB, Madka V, Brewer M, Ritchie RL, Lightfoot S, Kumar G, Sadeghi M, Patlolla JM, Yamada HY, Cruz-Monserrate Z, May R, Houchen CW, Steele VE and Rao CV. Targeting pancreatitis blocks tumor-initiating stem cells and pancreatic cancer progression. Oncotarget 2015; 6: 15524-15539.

[15] Schroeder CP, Yang P, Newman RA and Lotan R. Simultaneous inhibition of COX-2 and 5-LOX activities augments growth arrest and death of premalignant and malignant human lung cell lines. J Exp Ther Oncol 2007; 6: 183-192.

[16] Cicero AF and Laghi L. Activity and potential role of licofelone in the management of osteoarthritis. Clin Interv Aging 2007; 2: 73-79.

[17] Mohammed A, Janakiram NB, Li Q, Choi CI, Zhang Y, Steele VE and Rao CV. Chemoprevention of colon and small intestinal tumorigenesis in APC(Min/+) mice by licofelone, a novel dual 5-LOX/COX inhibitor: potential implications for human colon cancer prevention. Cancer Prev Res (Phila) 2011; 4: 2015-2026.

[18] Helgadottir A, Manolescu A, Thorleifsson G, Gretarsdottir S, Jonsdottir H, Thorsteinsdottir U, Samani NJ, Gudmundsson G, Grant SF,

Thorgeirsson G, Sveinbjornsdottir S, Valdimarsson EM, Matthiasson SE, Johannsson H, Gudmundsdottir O, Gurney ME, Sainz J, Thorhallsdottir M, Andresdottir M, Frigge ML, Topol EJ, Kong A, Gudnason V, Hakonarson H, Gulcher JR and Stefansson K. The gene encoding 5-lipoxygenase activating protein confers risk of myocardial infarction and stroke. Nat Genet 2004; 36: 233-239.

[19] Duffield-Lillico AJ, Boyle JO, Zhou XK, Ghosh A, Butala GS, Subbaramaiah K, Newman RA, Morrow JD, Milne GL and Dannenberg AJ. Levels of prostaglandin E metabolite and leukotriene E(4) are increased in the urine of smokers: evidence that celecoxib shunts arachidonic acid into the 5-lipoxygenase pathway. Cancer Prev Res (Phila) 2009; 2: 322-329.

[20] Jovanovic DV, Fernandes JC, Martel-Pelletier J, Jolicoeur FC, Reboul P, Laufer S, Tries S and Pelletier JP. In vivo dual inhibition of cyclooxygenase and lipoxygenase by ML-3000 reduces the progression of experimental osteoarthritis: suppression of collagenase 1 and interleukin-1beta synthesis. Arthritis Rheum 2001; 44: 2320-2330.

[21] Rainsford KD, Ying C and Smith F. Effects of 5-lipoxygenase inhibitors on interleukin production by human synovial tissues in organ culture: comparison with interleukin-1-synthesis inhibitors. J Pharm Pharmacol 1996; 48: 46-52.

[22] Babbar N and Gerner EW. Targeting polyamines and inflammation for cancer prevention. Recent Results Cancer Res 2011; 188: 49-64.

[23] Patlolla JM, Kopelovich L, Qian L, Zhang Y, Kumar G, Madka V, Mohammed A, Laura B, Sadeghi M, Lightfoot S and Rao CV. Early and Delayed Intervention with Rapamycin Prevents NNK-induced lung adenocarcinoma in A/J mice. Oncology Reports 2015; 34: 2925-2934.

[24] Nikitin AY, Alcaraz A, Anver MR, Bronson RT, Cardiff RD, Dixon D, Fraire AE, Gabrielson EW, Gunning WT, Haines DC, Kaufman MH, Linnoila RI, Maronpot RR, Rabson AS, Reddick RL, Rehm S, Rozengurt N, Schuller HM, Shmidt EN, Travis WD, Ward JM and Jacks T. Classification of proliferative pulmonary lesions of the mouse: recommendations of the mouse models of human cancers consortium. Cancer Res 2004; 64: 2307-2316.

[25] Kumar G, Tajpara P, Bukhari AB, Ramchandani AG, De A and Maru GB. Dietary curcumin post-treatment enhances the disappearance of B(a)P-derived DNA adducts in mouse liver and lungs. Toxicology Reports 2014; 1: 1181–1194.

[26] Kumar G, Tajpara P and Maru G. Dietary turmeric post-treatment decreases DMBA-induced hamster buccal pouch tumor growth by altering cell proliferation and apoptosis-related markers. J Environ Pathol Toxicol Oncol 2012; 31: 295-312.

[27] Kumar G, Dange P, Kailaje V, Vaidya MM, Ramchandani AG and Maru GB. Polymeric black tea polyphenols modulate the localization and activity of 12-O-tetradecanoylphorbol-13-acetate-mediated kinases in mouse skin: mechanisms of their anti-tumor-promoting action. Free Radic Biol Med 2012; 53: 1358-1370.

[28] Livak KJ and Schmittgen TD. Analysis of relative gene expression data using real-time quantitative PCR and the 2(-Delta Delta C(T)) Method. Methods 2001; 25: 402-408.

[29] Mohammed A, Janakiram NB, Brewer M, Vedala K, Steele VE and Rao CV. Multitargeted low-dose GLAD combination chemoprevention: a novel and promising approach to combat colon carcinogenesis. Neoplasia 2013; 15: 481-490.

[30] Nagase H and Woessner JF Jr. Matrix metalloproteinases. J Biol Chem 1999; 274: 21491-21494.

[31] Arumugam A, Weng Z, Talwelkar SS, Chaudhary SC, Kopelovich L, Elmets CA, Afaq F and Athar M. Inhibiting cycloxygenase and ornithine decarboxylase by diclofenac and alpha-difluoromethylornithine blocks cutaneous SCCs by targeting Akt-ERK axis. PLoS One 2013; 8: e80076.

[32] Saba NF, Hurwitz SJ, Kono SA, Yang CS, Zhao Y, Chen Z, Sica G, Muller S, Moreno-Williams R, Lewis M, Grist W, Chen AY, Moore CE, Owonikoko TK, Ramalingam S, Beitler JJ, Nannapaneni S, Shin HJ, Grandis JR, Khuri FR, Chen ZG and Shin DM. Chemoprevention of head and neck cancer with celecoxib and erlotinib: results of a phase ib and pharmacokinetic study. Cancer Prev Res (Phila) 2014; 7: 283-291.

[33] Sharma S, Lee J, Zhou J and Steele VE. Chemopreventive efficacy and mechanism of licofelone in a mouse lung tumor model via aspiration. Cancer Prev Res (Phila) 2011; 4: 1233-1242.

[34] Chang HH and Meuillet EJ. Identification and development of mPGES-1 inhibitors: where we are at? Future Med Chem 2011; 3: 1909-1934.

[35] Gerner EW and Meyskens FL Jr. Polyamines and cancer: old molecules, new understanding. Nat Rev Cancer 2004; 4: 781-792.

[36] Yamashita T, Nishimura K, Saiki R, Okudaira H, Tome M, Higashi K, Nakamura M, Terui Y, Fujiwara K, Kashiwagi K and Igarashi K. Role of polyamines at the G1/S boundary and G2/M phase of the cell cycle. Int J Biochem Cell Biol 2013; 45: 1042-1050.

[37] Levine AJ. p53, the cellular gatekeeper for growth and division. Cell 1997; 88: 323-331.
[38] Madka V, Mohammed A, Li Q, Zhang Y, Kumar G, Lightfoot S, Wu X, Steele V, Kopelovich L and Rao CV. TP53 modulating agent, CP-31398 enhances antitumor effects of ODC inhibitor in mouse model of urinary bladder transitional cell carcinoma. Am J Cancer Res 2015; 5: 3030-3041.
[39] Sedger LM and McDermott MF. TNF and TNF-receptors: From mediators of cell death and inflammation to therapeutic giants - past, present and future. Cytokine Growth Factor Rev 2014; 25: 453-472.
[40] Pine SR, Mechanic LE, Enewold L, Chaturvedi AK, Katki HA, Zheng YL, Bowman ED, Engels EA, Caporaso NE and Harris CC. Increased levels of circulating interleukin 6, interleukin 8, C-reactive protein, and risk of lung cancer. J Natl Cancer Inst 2011; 103: 1112-1122.
[41] Elaraj DM, Weinreich DM, Varghese S, Puhlmann M, Hewitt SM, Carroll NM, Feldman ED, Turner EM and Alexander HR. The role of interleukin 1 in growth and metastasis of human cancer xenografts. Clin Cancer Res 2006; 12: 1088-1096.
[42] Facchini A, Borzi RM, Marcu KB, Stefanelli C, Olivotto E, Goldring MB, Facchini A and Flamigni F. Polyamine depletion inhibits NF-kappaB binding to DNA and interleukin-8 production in human chondrocytes stimulated by tumor necrosis factor-alpha. J Cell Physiol 2005; 204: 956-963.
[43] Goetzl EJ, Banda MJ and Leppert D. Matrix metalloproteinases in immunity. J Immunol 1996; 156: 1-4.
[44] Boileau C, Pelletier JP, Tardif G, Fahmi H, Laufer S, Lavigne M and Martel-Pelletier J. The regulation of human MMP-13 by licofelone, an inhibitor of cyclo-oxygenases and 5-lipoxygenase, in human osteoarthritic chondrocytes is mediated by the inhibition of the p38 MAP kinase signalling pathway. Ann Rheum Dis 2005; 64: 891-898.
[45] Izbicka E, Streeper RT, Yeh IT, Pressley O, Grant M, Andrews JV, Kuhn J and O'Shaughnessy J. Effects of alpha-difluoromethylornithine on markers of proliferation, invasion, and apoptosis in breast cancer. Anticancer Res 2010; 30: 2263-2269.

Supplementary Table 1. Oligonucleotides for real-time PCR

Gene	Primer sequence	Accession number	Amplicon (bp)
Oat	5'-TGCCACCCAAAGATCATAGATGC-3' (F)	NM_016978.2	103
	5'-TGTACTCCTCGTATTCACCAAGG-3' (R)		
Oaz	5'-CTGAATGCTGTGTTTGTCAC-3' (F)	NM_001301034.1	97
	5'-GGTCACCTGACCATCTTAAA-3' (R)		
SAT1	5'-CCCTTGCTTTCTATCTTGTG-3' (F)	NM_009121.4	117
	5'-CATGACTGCCACTTTAAACA-3' (R)		
p53	5'-TGAAACGCCGACCTATCCTTA-3' (F)	NM_011640.3	92
	5'-GGCACAAACACGAACCTCAAA-3' (R)		
p21	5'-CGAGAACGGTGGAACTTTGAC-3' (F)	NM_007669.4	62
	5'-TCCCAGACGAAGTTGCCCT-3' (R)		
p27	5'-AGTGTCCCTTTCGGTAAGAATG-3' (F)	NM_009875.4	118
	5'-TCAGAACCTCCAAGTGAGAATAAG-3' (R)		
IL-1β	5'- CAACCAACAAGTGATATTCTCCATG-3' (F)	NM_008361.4	154
	5'- GATCCACACACTCTCCAGCTGCA-3' (R)		
IL-6	5'- TCCAGTTGCCTTCTTGGGAC-3' (F)	NM_001314054.1	74
	5'- AGTCTCCTCTCCGGACTTGT-3' (R)		
TNF-α	5'- AGAACTCCAGGCGGTGCCTATGT-3' (F)	NM_013693.3	209
	5'- GTGGGCTACAGGCTTGTCACTCG-3' (R)		
Cox-2	5'-TGAGCAACTATTCCAAACCAGC-3' (F)	NM_011198.4	74
	5'-GCACGTAGTCTTCGATCACTATC-3' (R)		
mPGES-1	5'-GAACGACATGGAGACCATCTAC-3' (F)	NM_022415.3	83
	5'-TCCAGGCGACAAAAGGGTTA-3' (R)		
FLAP	5'-GCCGGACTGATGTACCTGTT-3' (F)	NM_009663.2	259
	5'-GGTGAGCGTCCTTCTCTGTC-3' (R)		
LOX	5'-GGACCTCAGCATGTGGTATG-3' (F)	NM_009662.2	142
	5'-GCTGGGTCAGGGGTACTTTA-3' (R)		
PCNA	5'-TAAAGAAGAGGAGGCGGTAA-3' (F)	NM_011045.2	175
	5'-TAAGTGTCCCATGTCAGCAA-3' (R)		
MMP-2	5'-CCCTGTTCCCACGGGCCCTA-3' (F)	NM_008610.2	81
	5'-AGGAGGACAGAGCCGCCAGG-3' (R)		
MMP-7	5'-GGCAGCTATGCAGCTCACCCT-3' (F)	NM_010810.4	75
	5'-TCCTGGGACAGTGGCAGGGC-3' (R)		
MMP-9	5'-GCCGACTTTTGTGGTCTTCC-3' (F)	NM_013599.3	121
	5'-CTTCTCTCCCATCATCTGGGC-3' (R)		
MMP-13	5'-CAGGCACTGCTGGGCACCAT-3' (F)	NM_008607.2	82
	5'-GGGGCAGGGACCAACAGGGA-3' (R)		
Actin	5'-AGATCTGGCACCACACCTTC-3' (F)	NM_007393.4	139
	5'-GGGGTGTTGAAGGTCTCAAA-3' (R)		

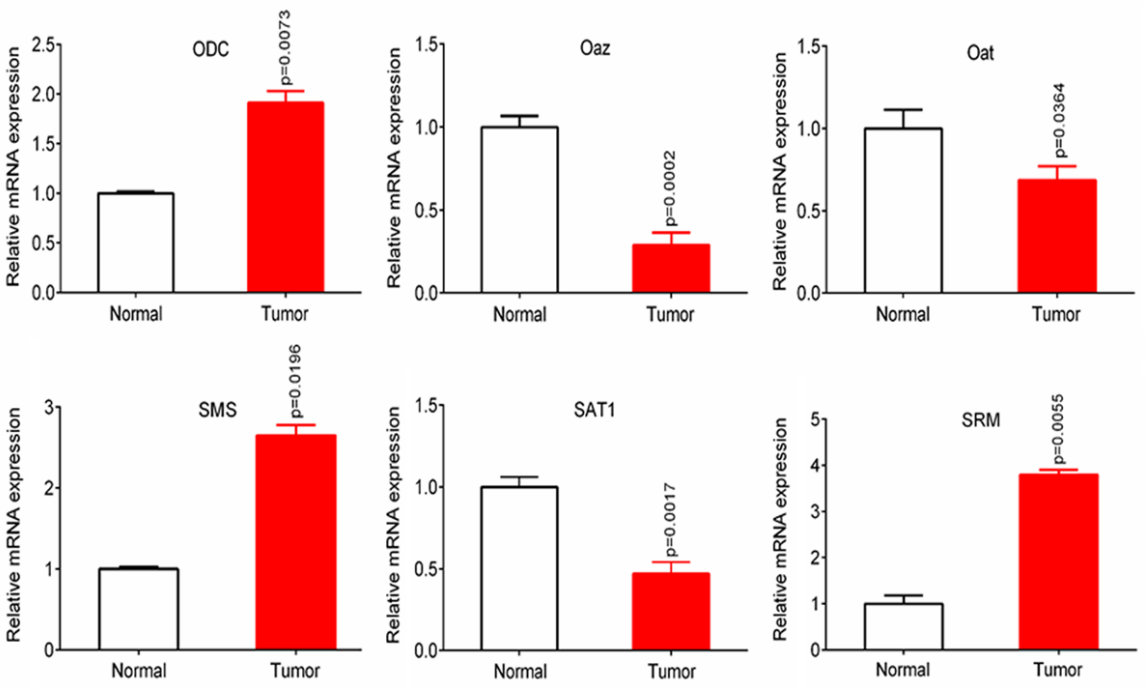

Supplementary Figure 1. Effect of DFMO, licofelone, and the combination on the polyamine synthesis pathway in normal and tumor lung tissue. Relative mRNA expression of ODC, Oaz, Oat, SMS, SAT, and SRM in RNA samples from different treatment groups as analyzed by real-time PCR and normalized to β-actin. Differences between control and treatment groups were analyzed by one-tailed *t*-test with Welch correction and 95% confidence interval. Data represent means ± *SE*. $p \leq 0.05$ was considered statistically significant.

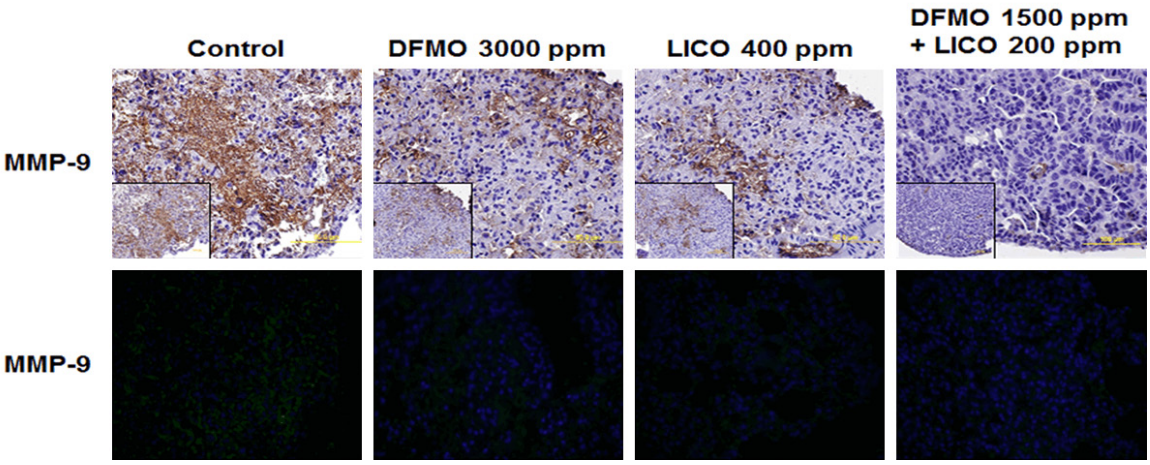

Supplementary Figure 2. Effect of DFMO, licofelone, and the combination on MMP-9. Representative photomicrographs showing IHC and IF of MMP-9 (magnification ×600; inset shows 400× magnification).